Fracton critical point at a higher-order topological phase transition

Yizhi You, Julian Bibo, Frank Pollmann, and Taylor L. Hughes

Phys. Rev. B **106**, 235130 — Published 15 December 2022

DOI: 10.1103/PhysRevB.106.235130

Fracton Critical Point at a Higher-Order Topological Phase Transition

Yizhi You,[1] Julian Bibo,[2,3] Frank Pollmann,[2,3] and Taylor L. Hughes[4]

[1]*Princeton Center for Theoretical Science, Princeton University, NJ, 08544, USA*
[2]*Department of Physics, Technical University of Munich, 85748 Garching, Germany*
[3]*Munich Center for Quantum Science and Technology (MQCST), D-80799 Munich, Germany*
[4]*Department of Physics and Institute for Condensed Matter Theory, University of Illinois at Urbana-Champaign, Illinois 61801, USA*

(Dated: October 5, 2022)

The theory of quantum phase transitions separating different phases with distinct symmetry patterns at zero temperature is one of the foundations of modern quantum many-body physics. Here we demonstrate that the existence of a 2D topological phase transition between a higher-order topological insulator (HOTI) and a trivial Mott insulator with the same symmetry eludes this paradigm. We present a theory of this quantum critical point (QCP) driven by the fluctuations and percolation of the domain walls between a HOTI and a trivial Mott insulator region. Due to the spinon zero modes that decorate the rough corners of the domain walls, the fluctuations of the phase boundaries trigger a spinon-dipole hopping term with fracton dynamics. Hence we find the QCP is characterized by a critical dipole liquid theory with subsystem $U(1)$ symmetry and the breakdown of the area law entanglement entropy which exhibits a logarithmic enhancement: $L\ln(L)$. Using the density matrix renormalization group (DMRG) method, we analyze the dipole stiffness together with the structure factor at the QCP which provide strong evidence of a critical dipole liquid with a Bose surface, UV-IR mixing, and a dispersion relation $\omega = k_x k_y$.

After a decade of intense effort focused on topological materials, a new class of symmetry protected topological insulators, dubbed Higher-Order Topological Insulators (HOTI) has been discovered [1–4]. HOTIs admit gapped surfaces separated by gapless corners/hinges where the surfaces intersect, and exemplify a rich bulk-boundary correspondence. Aside from HOTIs generated by topological band structures, recent research suggests strongly interacting bosonic systems can potentially host a HOTI having robust bosonic corner zero-modes [5, 6]. Now the characterization of interacting HOTIs has been widely-explored in terms of mathematical invariants, topological response, and field theory approaches [7, 8]. However, the existence and character of a quantum phase transition between an interacting HOTI phase and a trivial Mott insulator phase is still nebulous. In particular, it is noteworthy to explore whether the critical region inherits the topological properties of the HOTI, and how such a phase transition is influenced by the topological structure, and the entanglement pattern, of the adjacent HOTI phase.

In this work, we address these questions and propose a new type of quantum critical point that connects a 2D HOTI phase [8, 9] and a trivial Mott insulator phase. The traditional guiding principle behind the modern theory of critical phenomena, known as the Ginzburg-Landau-Wilson (GLW) paradigm, is the identification of an 'order parameter fluctuation' that encapsulates the differences in symmetry between the two phases proximate to the critical point. However, the quantum critical point (QCP) we present in this paper eludes this paradigm as both the HOTI phase, and the trivial Mott phase, have the same symmetries, and are distinguished through only their different topological character.

Remarkably, we find that the phase transition we propose inherits topological features from the HOTI phase. The QCP can be understood as the bulk percolation [10] of domain walls that act as phase boundaries between regions containing HOTI or trivial Mott insulator. The corners and rough patches of the 1D domain walls can be treated as the corners of the HOTI phase, and are thus each decorated with a robust spinon zero mode. At the QCP, the proliferation of domain walls triggers the fluctuations of the corner zero modes, and precipitates fracton dynamics of the spinons that are constrained by subsystem $U(1)$ symmetry. Hence, we find that this critical point contains quasiparticles with fracton behavior and sub-dimensional kinetics where the spinon-dipoles only move transverse to their dipole moment [11–28]. This new type of quantum criticality leads us to propose that the phase transition is characterized by a critical dipole liquid [25, 29–32]. This critical theory has several key features including: (i) a Bose surface [33] having zero energy states that form closed nodal-lines along the k_x and k_y axes, and (ii) a breakdown in the area law of the entanglement entropy, which is replaced by a scaling with a logarithmic enhancement $L\ln(L)$ at the critical point instead. (iii) The phase transition theory is subject to UV-IR mixing as the critical point is controlled by short-wave length modes with strong local fluctuations.

To frame our discussion we consider the following model on a 2D square lattice with four spin-1/2 degrees of freedom per unit cell:

$$\begin{aligned} H &= H_{XY} - \lambda H_{\text{ring exchange}} \\ &= \sum_{\mathbf{R}} \left(S^+_{\mathbf{R},1} S^-_{\mathbf{R},2} + S^+_{\mathbf{R},2} S^-_{\mathbf{R},3} + S^+_{\mathbf{R},3} S^-_{\mathbf{R},4} + S^+_{\mathbf{R},4} S^-_{\mathbf{R},1} \right) \\ &- \lambda \sum_{\mathbf{R}} \left(S^+_{\mathbf{R},2} S^-_{\mathbf{R}+\mathbf{e}_x,1} S^+_{\mathbf{R}+\mathbf{e}_x+\mathbf{e}_y,4} S^-_{\mathbf{R}+\mathbf{e}_y,3} \right) + h.c. \end{aligned} \tag{1}$$

Hamiltonian (1) contains an inter-cell ring-exchange interaction between the four spins located at the four corners of each red plaquette, and an XY spin interaction within the unit cell as shown in Fig. 1(a). In passing we mention that models having ring-exchange terms of this type can be realized in cold-atom settings, which hence is a natural arena for experimental investigation of our subsequent predictions [34, 35]. The magnon creation/annihilation operators $S^{\pm} = \sigma^x \pm i\sigma^y$ can be mapped to a hardcore boson description using $b^\dagger(b) = S^+(S^-), S^z = n_b - 1/2$, where $n_b = b^\dagger b$; we use both languages interchangeably where convenient. Eq. (1) exhibits time-reversal $\mathcal{T} = \prod_{\mathbf{R}} \prod_{m=1}^4 i\sigma^y_{\mathbf{R},m} \mathcal{K}$ symmetry and a subsystem U(1) symmetry that conserves the sum of S^z inside the unit cell $\mathbf{R}$, i.e. $S^z(\mathbf{R}) = \sum_{m=1}^4 S^z_{\mathbf{R},m}$, for every row (R) and column (C),

$$U^{\text{sub}}_{R(C)}(1) : \prod_{\mathbf{R} \in R(C)} e^{i\theta S^z(\mathbf{R})}. \tag{2}$$

The subsystem U(1) symmetry restricts the mobility of the magnon, hence the leading order dynamics are attributed to pairs of dipoles, each composed of a particle-hole pair on a lattice link, that hop along the direction transverse to their dipole moment.

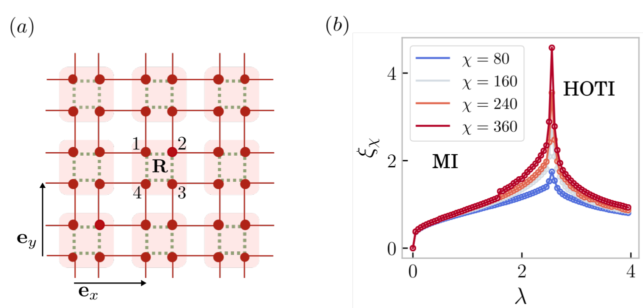

FIG. 1. **Lattice model and quantum critical point (QCP).** Panel (a) shows the lattice model. Each unit cell consists of four spin $S = 1/2$ (red dots). The ring-exchange terms (red squares) couple four neighboring unit cells, while sites in the unit cell are isotropically coupled via an XY interaction (green dotted lines). Panel (b) shows the correlation length ξ_χ as function of the tuning parameter λ and the bond dimension χ for an infinite cylinder along x, $L_x = \infty$, and periodic boundary conditions along y with a circumference $L_y = 6$. A second order quantum phase transition between a Mott-Insulator (MI) and higher order topological insulator (HOTI) occurs at $\lambda_c \approx 2.54$.

Before turning to the detailed study of the phase diagram for the model Eq. (1), let us discuss two exactly solvable limits. As λ is tuned, the system effectively has competing orders dominated by either the intra-cell XY interaction, or the inter-cell plaquette ring-exchange interaction. In the limit $\lambda \sim 0$, the intra-cell term plays the key role and generates an entangled cluster within each unit cell. The resulting ground state, which is simply a tensor product of the ground state of each unit cell, is a featureless Mott insulator with a magnon gap for both the bulk and boundary. In the opposite limit $\lambda \sim \infty$, it was shown in Ref. [8] that the plaquette term projects the four interacting spins into a unique maximally entangled state $|\downarrow_2\uparrow_1\downarrow_4\uparrow_3\rangle + |\uparrow_2\downarrow_1\uparrow_4\downarrow_3\rangle$ where we omitted unit cell labels. The corresponding ground state for the entire system is thus a product of entangled plaquettes, and has a finite magnon gap in the bulk. In the presence of a smooth boundary, each edge unit cell naively has two free spin-1/2 modes, but these can be coupled and gapped to form a singlet state via the onsite XY coupling in Eq. (1) (even for infinitesimal λ). For rough edges and/or corners, there is an additional spin-1/2 zero mode per corner whose two-fold degeneracy is protected by both $\mathcal{T}$ and subsystem U(1) symmetry so the resultant state renders a higher-order topological insulator. This subsystem symmetric HOTI phase was studied in Ref. [8], and was shown to exhibit a quantized quadrupole moment density of $Q_{xy} = 1/2$.

We obtained the phase diagram, Fig. 1(b) using the DMRG method [36–38] on an infinitely long cylinder. We find that the aforementioned limits extend into two gapped phases (a trivial Mott insulator and a HOTI respectively). Importantly, our numerics indicate that the two gapped phases are connected by a second-order phase transition at $\lambda_c \approx 2.54$. It is noteworthy to emphasize that the HOTI phase and the trivial Mott phase display the same symmetries, but harbor distinct topological features, and thus cannot be differentiated via any local observable. This further implies that the QCP between the phases is beyond the GLW paradigm.

We now provide both an analytic argument and numerical evidence to demonstrate that the quantum critical point separating the HOTI phase and the trivial Mott phase displays gapless fracton quasi-particles akin to a critical dipole liquid. When the interaction strength λ is comparable to the intra-cell tunneling strength, the plaquette entangled patterns and on-site entangled patterns compete and coexist in the bulk. The coexistence and spatial phase separation can be viewed from a percolation picture illustrated in Fig. 2. In the quantum critical region adjacent to the trivial Mott phase, the plaquette ring-exchange term triggers some regions containing plaquette entangled states that exhibit the HOTI ground state pattern. Domain walls that form between the two phases can be viewed as the boundary between the HOTI and trivial phases, and hence they harbor a spinon zero mode at each corner (and each 'rough' patch on the edges). In the quantum critical region, strong fluctuations between different phase separation patterns are induced, and the domain walls tend to proliferate. These spatial fluctuations concurrently trigger the dynamics of the spinon zero modes on the corners of the domain walls, similar to the percolation of domain wall defects in 1D [10].

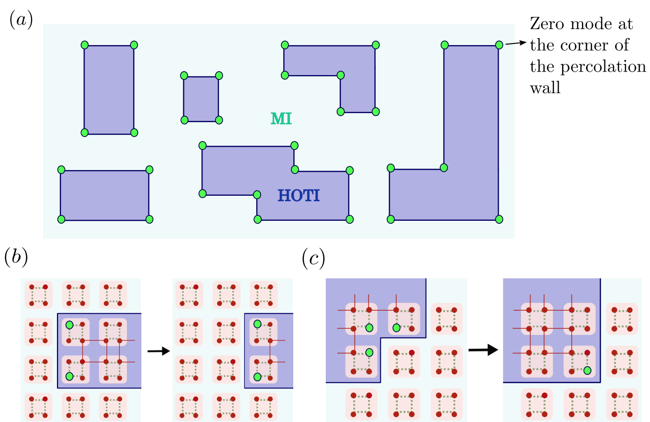

FIG. 2. (a) At the critical point, the HOTI (blue shaded area) and trivial Mott insulator (green shaded region) coexist and their phase boundary (domain wall) contains spinon zero modes (green dot) at the corners. (b)-(c) The spatial fluctuation of phase boundaries (domain walls) induces motion for the spinon-pairs at neighboring corners.

More precisely, the spinon dynamics originates from the resonance between distinct percolation patterns. In Figs. 2(b) and (c) we display two typical phase boundary deformations. By shrinking a stripe domain along the x-direction, the two spinon zero modes forming an effective y-oriented dipole can hop along the x-direction, and vice-versa. This motion can be described by a ring exchange term for the spinons:

$$\sum_{i=1}^{2} z_i^\dagger(\mathbf{R}) z_i(\mathbf{R}+\mathbf{e}_x) z_i^\dagger(\mathbf{R}+\mathbf{e}_x+\mathbf{e}_y) z_i(\mathbf{R}+\mathbf{e}_y), \quad (3)$$

where $(z_1^\dagger, z_2^\dagger)$ is the CP^1 representation of the spinon with $S_i^z = \frac{1}{2} z_i^\dagger \sigma_{ij}^z z_j$. Another typical domain wall deformation occurs when a corner is shrunk by removing a corner plaquette from the stripe. This effectively removes the free spinon from the corner, but it also creates three other spinons at the newly created corners. This process is also represented by the ring-exchange term in Eq. 3. Hence, the spatial fluctuations of the percolating domain walls generate a ring-exchange type term for spinons that effectively corresponds to the motion of dipoles transverse to their dipole moment. An important characteristic of this transition is that the percolation at the QCP does not trigger the hopping of a single spinon, stemming from the fact that the spinon modes on the phase boundaries are localized at the corners.

Based on these key observations, we propose that the low energy effective description of the QCP is a critical dipole liquid theory:

$$\mathcal{L} = \sum_{\gamma=1,2} (\partial_t \theta_\gamma + a_0)^2 - K(\partial_x \partial_y \theta_\gamma + a_{xy})^2,$$
$$a_{xy} \to a_{xy} + \partial_x \partial_y \alpha, \; a_0 \to a_t + \partial_t \alpha, \;\; z_i^\dagger = n_i e^{i\theta_i}. \quad (4)$$

Here we used a number-phase representation for the CP^1 spinons, and a_0, a_{xy} are components of the emergent gauge field that couple to the gauge charge of the spinon; their gauge transformations are also listed above. We note that we are ignoring the compactification of the boson fields θ_i, and have expanded to quadratic order in them [25]. The legitimacy of this approximation, which is tied to the irrelevance of instanton tunneling events, is discussed in detail in the Supplementary material. To further analyze this theory, we can decompose the two CP^1 phase fields as $\theta_\pm = \theta_1 \pm \theta_2$ to find:

$$\mathcal{L} = \frac{1}{2} \sum_{\gamma=\pm} (\partial_t \theta_\gamma)^2 - \frac{K}{2} (\partial_x \partial_y \theta_+ + a_{xy})^2 - \frac{K}{2} (\partial_x \partial_y \theta_-)^2. \quad (5)$$

We find that the field θ_+ is the only bosonic spinon mode that couples to the emergent gauge field a_{xy}. Hence this mode is gapped out due to a Higgs-like mechanism for the gauge field, or equivalently, by the onsite XY interaction (see Appendix for details). The field θ_- denotes the gapless magnon mode: $S^\pm = e^{i\pm\theta_-}$ that carries the S_z quantum number. This field contributes to the low energy dynamical phenomena at quantum criticality, and henceforth we only focus on the θ_- branch.

Due to subsystem S_z conservation, the action in Eq. (5) is invariant under a special U(1) transformation $\theta_- \to \theta_- + f(x) + g(y)$. Consequently, the single magnon hopping term $(\partial_i \theta_-)^2$ is forbidden as it breaks this subsystem U(1) symmetry explicitly. Instead, the leading order dynamics originates from dipole moments oriented along the i-th direction, i.e., $(\partial_i \theta_-)$ that are constrained to move along the transverse j-th direction. This is captured in our theory by a special, higher order kinetic term $(\partial_j \partial_i \theta_-)^2$ yielding a dispersion $\omega \sim k_x k_y$. This is remarkable because we find that the QCP exhibits characteristic fractonic features arising from a percolation process where the corner-localized low-energy modes cannot fluctuate independently without creating additional corners. Finally, we note that this theory can also be used to describe the gapped phases proximate to the QCP (see Supplement for details).

An alternative way to illustrate the fracton dynamics at the critical point is to explore the magnon dynamics directly from the microscopic Hamiltonian in Eq. (1). When the interaction strength λ grows, the inter-cell coupling term triggers the magnons to fluctuate between unit cells. However, as the inter-cell coupling contains only a ring exchange term, it does not support single charge hopping between cells, and hence the leading order dynamics is governed by a pair of magnon-dipoles hopping between cells [30, 31, 39, 40]. To corroborate this we find that the two point correlator $\langle S^+(\mathbf{R})S^-(\mathbf{R})\rangle$ is short ranged at the QCP. In contrast, since we expect that the critical region manifests a critical dipole liquid, we find that the four-point correlation functions between two spin-dipoles living on the same transverse stripe, exhibit [25]:

$$\langle S^+(\mathbf{R})S^-(\mathbf{R}+\mathbf{e}_y)S^-(\mathbf{R}+x)S^+(\mathbf{R}+x+\mathbf{e}_y)\rangle = \frac{1}{(x)^{1/(K\pi^2)}}, \tag{6}$$

and analogously for a stripe along y. These correlation functions exhibit algebraic decay and quasi-long range order if and only if the two dipoles are living on the same stripe. This again supports the fact that we should interpret the critical point as a dipole liquid having constrained subsystem dynamics.

As a further confirmation of the dipole liquid critical point, we characterize the dipole liquid by its transport properties since our model has dipole conservation. In the language of Ref. [41], we expect the critical dipole liquid to act as a 'dipole metal' and exhibit a non-vanishing dipole conductivity in the presence of a uniform rank-2 electric field, e.g., E_{xy}. In analogy to Kohn's criterion on defining conductors and insulators [42], Ref. [41] proposed a criterion to establish the existence of a dipole metal based on the dipole stiffness D_d (details of its definition and calculation can be found in the Supplement) suggesting that if D_d is non-vanishing in the thermodynamic limit, then the system is a dipole metal. Our results for D_d are shown in Fig. 3(b), and we find that they clearly support our theory since the system shows a non-vanishing D_d only in the neighborhood of the critical point.

Now let us consider several remarkable properties of this critical point. The critical theory in Eq. (5) produces a quadratic dispersion $\omega \sim k_x k_y$, which implies a Bose surface with characteristic lines of zero energy modes on both the k_x and k_y axes. For each fixed momentum slice $k_i \neq 0$, the low energy dispersion is akin to the 1D relativistic boson along the transverse direction. Such 'quasi-1D' motion is a consequence of the sub-dimensional nature of the critical dipole liquid, i.e., the fact that an $x(y)$-oriented dipole is only mobile along the transverse $y(x)$-oriented stripes. To confirm the existence of the Bose surface we numerically evaluate the structure factor:

$$S(\mathbf{q}) = \frac{1}{N}\left[\prod_{m=1}^{2}\sum_{\mathbf{R}_m,\mathbf{b}_m} e^{i\mathbf{q}\cdot[(-1)^m\mathbf{\Lambda}_m]}\right]\langle S^z_{\mathbf{\Lambda}_1} S^z_{\mathbf{\Lambda}_2}\rangle\,, \tag{7}$$

where $N = L_y L_x/4$ is the total number of unit cells, $\mathbf{\Lambda}_m = \mathbf{R}_m + \mathbf{b}_m$ specifies one the four spins $S^z_{\mathbf{R}_m,m}$ inside the unit cell $\mathbf{R}_m$ with basis vectors $\mathbf{b}_m \in \frac{1}{2}\{\mathbf{0}, \mathbf{e}_x, \mathbf{e}_y, \mathbf{e}_x + \mathbf{e}_y\}$. In Fig. 3(a) we show that the numerically obtained structure factor exhibits clear zero-energy lines along the k_x, k_y axes. Furthermore, each $k_i \neq 0$ exhibits dispersion like a 1D relativistic boson along the transverse direction. We note that since there are nodal lines at $k_x, k_y = 0$, there is a sub-extensive number of quasi-1D modes, and the specific heat at low temperature will scale as $C_v \sim T\ln(1/T)$, which is similar to marginal Fermi liquid theory in 2D [25, 29, 30]. Remarkably, as a subextensive number of zero energy modes survive at high momentum, the resultant theory is controlled and crucially depends on short wave-length modes that generate strong local fluctuations. Such a critical theory is triggered by short-wave length physics and is subject to UV-IR mixing[40](See Supplement for more details).

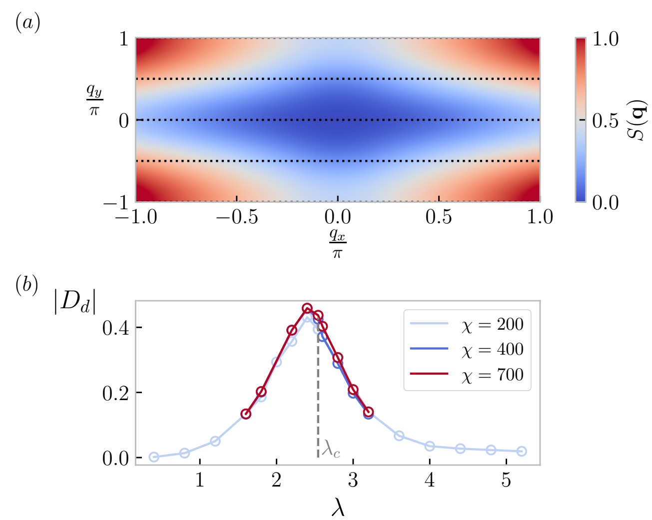

FIG. 3. **Static structure factor and dipole stiffness.** (*a*) The static structure factor $S(\mathbf{q})$ calculated for a stripe with $L_x = 100$ and $L_y = 8$ sites along the x and y direction, respectively. Hence, the data are obtained for momenta $q_y = 0, \pm\pi, \pm\pi/2$ (black, dotted lines). (*b*) The absolute value of the dipole stiffness $|D_d|$, calculated for an infinite cylinder with $L_y = 6$. The dipole stiffness is obtained by taking the second, symmetric derivative with step size $\delta\Phi = 0.05$.

Indeed, another noteworthy feature for the critical dipole liquid is an unusually large entanglement entropy scaling that exceeds the area law. In conventional 2D quantum critical points, despite the divergent correlation length, the entanglement entropy of the ground state carried by a sub-region of the many-body system is still local in the sense that it scales with L, the perimeter of the subsystem boundary. However, in the critical theory we present here, the entanglement entropy should scale with the sub-region size as $L\ln(L)$ [43, 44]. Such a violation of the area law can be substantiated by dividing the Bose surface into small patches over which the surface looks approximately flat. Each patch can be regarded as a 1D relativistic boson whose entanglement entropy scales as

$\ln(L)$. Summing over the contributions from all patches, the total entanglement entropy should scale as $L\ln(L)$. To our knowledge, this is the first observation of a 2D quantum critical point whose entanglement pushes beyond the area law. This implies that the critical dipole liquid has long range mutual information shared by two regions far apart.

In conclusion, we provided a framework to describe a novel type of 2D quantum criticality with logarithmic entanglement scaling and emergent fracton dynamics in the absence of Lorentz invariance. Our description of the HOTI percolation transition also suggests new insights for various topological phase transitions and critical points beyond the GLW paradigm, and is certain to have rich theoretical and experimental implications perhaps in near-term cold-atom experiments.

This work is initiated at KITP and YY, TLH, FP are supported in part by the National Science Foundation under Grant No. NSF PHY- 1748958(KITP) during the Topological Quantum Matter program. FP acknowledges the support of the DFG Research Unit FOR 1807 through grants no. PO 1370/2-1, TRR80, and the Deutsche Forschungsgemeinschaft (DFG, German Research Foundation) under Germany's Excellence Strategy EXC-2111-390814868. TLH thanks the US National Science Foundation (NSF) MRSEC program under NSF Award Number DMR-1720633 (SuperSEED) and the award DMR 1351895-CAR for support.

[1] W. A. Benalcazar, B. A. Bernevig, and T. L. Hughes, Science **357**, 61 (2017).
[2] F. Schindler, A. M. Cook, M. G. Vergniory, Z. Wang, S. S. Parkin, B. A. Bernevig, and T. Neupert, arXiv preprint arXiv:1708.03636 (2017).
[3] J. Langbehn, Y. Peng, L. Trifunovic, F. von Oppen, and P. W. Brouwer, Physical review letters **119**, 246401 (2017).
[4] Z. Song, Z. Fang, and C. Fang, Physical review letters **119**, 246402 (2017).
[5] Y. You, T. Devakul, F. J. Burnell, and T. Neupert, Physical Review B **98**, 235102 (2018).
[6] O. Dubinkin and T. L. Hughes, arXiv preprint arXiv:1807.09781 (2018).
[7] A. Rasmussen and Y.-M. Lu, arXiv preprint arXiv:1809.07325 (2018).
[8] Y. You, F. Burnell, and T. L. Hughes, arXiv preprint arXiv:1909.05868 (2019).
[9] J. Bibo, I. Lovas, Y. You, F. Grusdt, and F. Pollmann, arXiv preprint arXiv:1911.04149 (2019).
[10] X. Chen, F. Wang, Y.-M. Lu, and D.-H. Lee, Nuclear Physics B **873**, 248 (2013).
[11] C. Chamon, Physical review letters **94**, 040402 (2005).
[12] J. Haah, Phys. Rev. A **83**, 042330 (2011).
[13] B. Yoshida, Physical Review B **88**, 125122 (2013).
[14] S. Vijay, J. Haah, and L. Fu, Physical Review B **94**, 235157 (2016).
[15] M. Pretko, X. Chen, and Y. You, arXiv preprint arXiv:2001.01722 (2020).
[16] H. Ma, E. Lake, X. Chen, and M. Hermele, Physical Review B **95**, 245126 (2017).
[17] M. Pretko and L. Radzihovsky, arXiv preprint arXiv:1711.11044 (2017).
[18] M. Pretko, Physical Review B **96**, 035119 (2017).
[19] M. Pretko, Physical Review B **95**, 115139 (2017).
[20] D. Bulmash and M. Barkeshli, arXiv preprint arXiv:1806.01855 (2018).
[21] A. Gromov, A. Lucas, and R. M. Nandkishore, Physical Review Research **2**, 033124 (2020).
[22] A. Gromov, Physical Review X **9**, 031035 (2019).
[23] H. Ma and M. Pretko, Physical Review B **98**, 125105 (2018).
[24] W. Shirley, K. Slagle, and X. Chen, arXiv preprint arXiv:1806.08625 (2018).
[25] Y. You, Z. Bi, and M. Pretko, arXiv preprint arXiv:1908.08540 (2019).
[26] A. Prem, M. Pretko, and R. Nandkishore, arXiv preprint arXiv:1709.09673 (2017).
[27] R. M. Nandkishore and M. Hermele, Annual Review of Condensed Matter Physics **10**, 295 (2019).
[28] J. Feldmeier, P. Sala, G. De Tomasi, F. Pollmann, and M. Knap, Physical Review Letters **125**, 245303 (2020).
[29] C. Xu and M. P. Fisher, Physical Review B **75**, 104428 (2007).
[30] A. Paramekanti, L. Balents, and M. P. Fisher, Physical Review B **66**, 054526 (2002).
[31] T. Tay and O. I. Motrunich, Physical review letters **105**, 187202 (2010).
[32] R. V. Mishmash, M. S. Block, R. K. Kaul, D. Sheng, O. I. Motrunich, and M. P. Fisher, Physical Review B **84**, 245127 (2011).
[33] S. Sachdev, Nature **418**, 739 (2002).
[34] B. Paredes and I. Bloch, Phys. Rev. A **77**, 023603 (2008).
[35] H.-N. Dai, B. Yang, A. Reingruber, H. Sun, X.-F. Xu, Y.-A. Chen, Z.-S. Yuan, and J.-W. Pan, Nat. Phys. **13**, 1195 (2017).
[36] S. R. White, Physical Review Letters **69**, 2863 (1992).
[37] I. P. McCulloch, arXiv:0804.2509 (2008).
[38] J. Hauschild and F. Pollmann, SciPost Phys. Lect. Notes (2018).
[39] C. D. Batista and Z. Nussinov, Phys. Rev. B Condens. Matter **72**, 045137 (2005).
[40] N. Seiberg and S.-H. Shao, arXiv preprint arXiv:2004.00015 (2020).
[41] O. Dubinkin, J. May-Mann, and T. L. Hughes, arXiv preprint arXiv:1909.07403 (2019).
[42] W. Kohn, Phys. Rev. **133**, A171 (1964).
[43] H.-H. Lai, K. Yang, and N. E. Bonesteel, Phys. Rev. Lett. **111**, 210402 (2013).
[44] B. Swingle, Phys. Rev. Lett. **105**, 050502 (2010).